S1. Statistical evaluation of the experimental design

S1.1 2^3 full factorial design with three centerpoints

The phenomenon observed when analyzing the first set of experiments is the so called critical mix. In this case some of the results show a behavior that is qualitatively different from the others and thus it is not sensible to fit a smooth mathematical model for the data even though it would be operationally possible. The correct course of action in this case is to find a region in the factor space where this irregular behavior is not observed. Interaction plots (Fig. S1) show typical shapes when a critical mix is encountered.

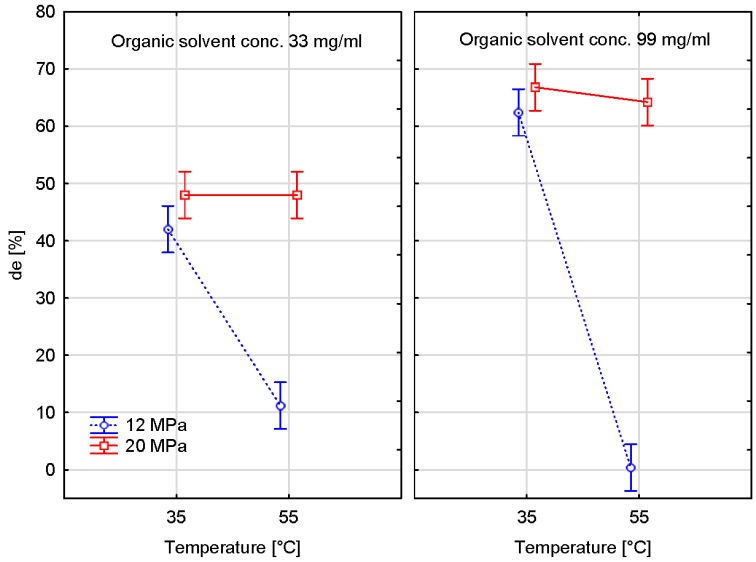

Fig. S1 Interaction plots showing the effects of pressure, temperature and organic solvent concentration on the diastereomeric excess

S1.2. Experimental design with the discontinuous part removed and the additional points added

With the data points removed and added, this experimental design is not orthogonal anymore. This means that the different effects are confounded with each other and they cannot be estimated independently.

The following model was fitted for the diastereomeric excess:

$$f(x_1; x_2; x_3) = b_0 + b_1x_1 + b_2x_2 + b_3x_3 + b_{11}x_1^2 + b_{22}x_2^2 + b_{12}x_1x_2 + b_{13}x_1x_3 + b_{23}x_2x_3$$

Where $f(x_1; x_2; x_3)$ denotes the variable, the value of which is estimated, while x_1, x_2 and x_3 stand for the levels of the chosen factors. Table S1 contains the fitted parameters for the diastereomeric excess according to a full model. The model for the diastereomeric excess was reduced stepwise based on effect sparsity and the reduced model can be seen in Table S2.

Table S1 The fitted parameters for the diastereomeric excess (full model)

Factor	Coeff.	Std. Err. Coeff.	-95% Cnf. Limt	+95% Cnf. Limt	p
Mean/Interc.	59.2667	0.54569	56.919	61.6146	0.000085
(1)Pressure [MPA](L)	41.9500	14.58127	-20.788	104.6881	0.102564
Pressure [MPA](Q)	2.2000	5.08010	-19.658	24.0579	0.707199
(2)Temperature [°C](L)	-40.0000	14.47751	-102.292	22.2917	0.109835
Temperature [°C](Q)	-46.6667	19.42126	-130.230	36.8963	0.138185
(3) Organic solvent conc. [mg/ml](L)	9.1500	0.47258	7.117	11.1834	0.002657
1L by 2L	39.3500	14.47751	-22.942	101.6417	0.112897
1L by 3L	-0.4000	0.47258	-2.433	1.6334	0.486447
2L by 3L	-0.6500	0.47258	-2.683	1.3834	0.302793

Table S2 The fitted parameters for the diastereomeric excess (reduced model)

Factor	Coeff.	Std. Err. Coeff.	-95% Cnf. Limt	+95% Cnf. Limt	p
Mean/Interc.	59.26667	1.110361	56.64108	61.89225	0.000000
(1)Pressure [MPA](L)	2.51786	0.703820	0.85359	4.18213	0.009007
(3) Organic solvent conc. [mg/ml](L)	9.07143	0.726902	7.35258	10.79028	0.000005
Organic solvent conc. [mg/ml](Q)	-5.03452	1.314635	-8.14314	-1.92591	0.006461

S2. Solid state investigation of the crystal structure: powder X-ray diffraction

Powder X-ray diffraction investigations were done on a PANalytical 'Xpert Pro diffractometer. It is equipped with an X'celerator detector. The wavelength of the X-ray was 1.5408 Å (Cu Kα) and 40 kV and 30 mA were applied to the X-ray tube. Scanning was performed between the 2Θ angles of 4 and 46°, with a total scanning time of 10 min.

Fig. S2 shows a comparison of the diffractograms of the diastereomeric salt samples obtained in the initial resolution step, the raffinate samples from the further purification experiments and the references obtained from the Cambridge Structural Database [1], using the computer program Mercury [2]. They are powder diffractograms of the more stable [3, 4] and less stable [5, 6] diastereomeric salts, calculated from the atomic positions obtained from single crystal investigations.

While the characteristic lines at low 2Θ angles (corresponding to more distant crystal-lattices) of the samples obtained from this study match those of the literature references quite accurately, some new peaks can be discovered at higher 2Θ angles. As the capillary electrophoresis measurements showed no detectable contaminant in the samples, one can assume that these diffraction lines might belong to polymorphs of the 1-phenylethanammonium-mandelate salts that are present in detectable but very low amounts in the samples. Further investigations would be needed to confirm the origin of these lines. However, the diffraction patterns, thus the crystal structure and the nature of the half-molar equivalent resolution raffinates and the crystalline products of the further purification experiments are very similar.

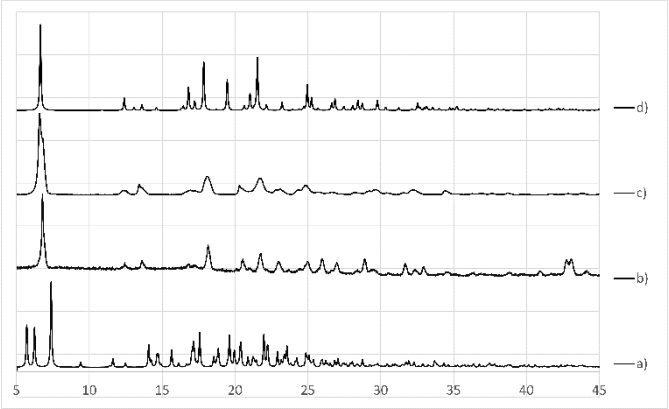

Fig. S2 Comparison of the powder XRD patterns of the products and literature references. a) The pattern of the less stable (*S*)-phenylethylammonium-(*R*)-mandelate salt [5, 6] b) The diffraction pattern of a raffinate from a resolution using half molar equivalent of (*R*)-phenylethylamine (*de*=64%) c) The raffinate of a further purification experiment (*de*=92%) d) Pattern of the more stable (*R*)-1-phenylethylammonium-(*R*)-mandelate [3, 4]

S3. Scanning electron microscopy images

Scanning electron microscopy images of the raffinate sample obtained at 12 MPa, 35 °C and 99 mg/ml were recorded using a JEOL JSM 5500-LV scanning electron microscope and a secondary electron detector. An acceleration voltage of 20 kV was applied. In order to make the surface of the samples conductive, they were coated with a Au-Pd layer having a thickness of approx. 10 nm. In Fig. S3, the sheet-like shapes of the crystals can be observed as well as the length and width ranges. The particles were found to be roughly 2 µm to 25 µm wide and approximately 20 µm and 140 µm long.

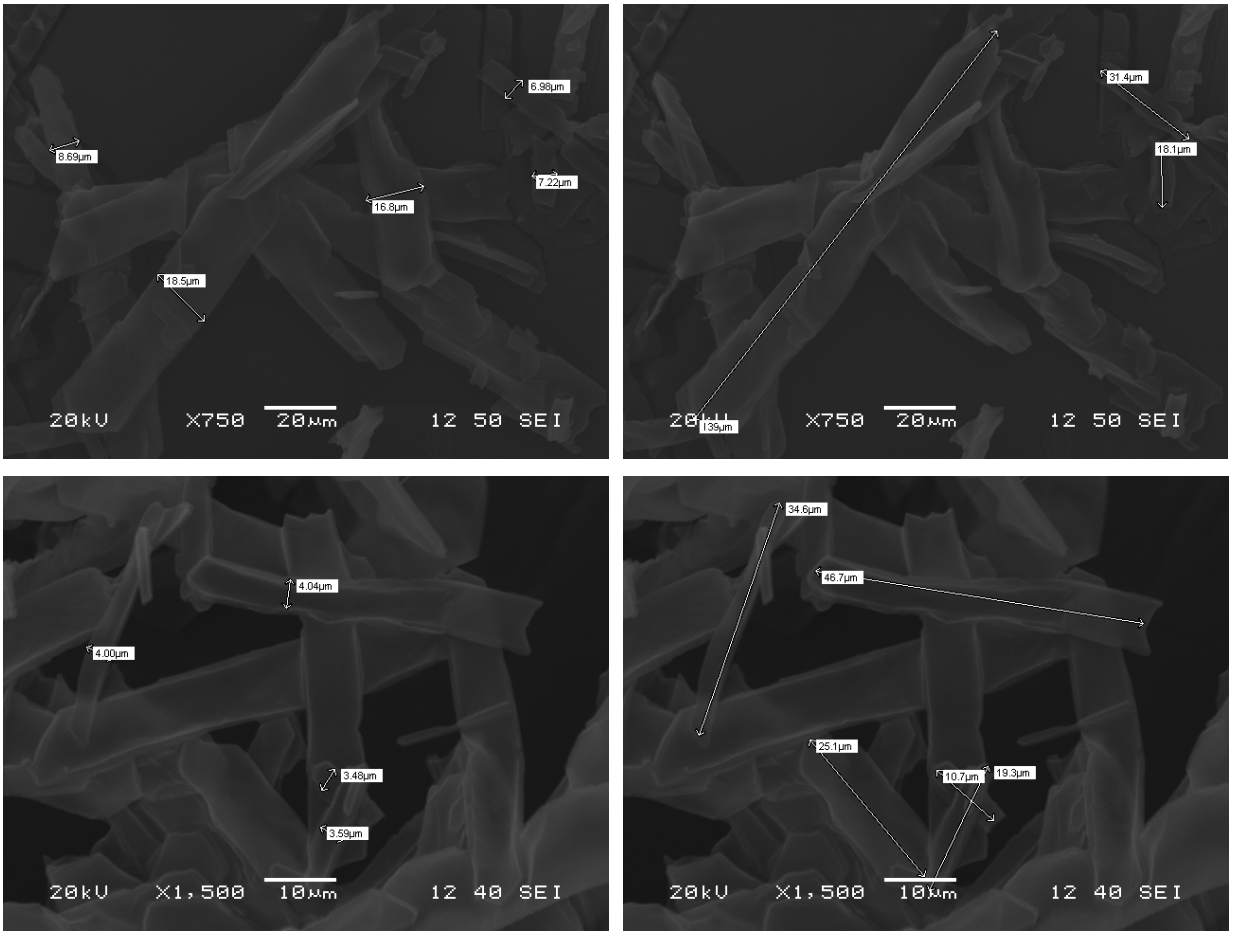

Fig. S3 Scanning electron microscopy images of the raffinate obtained in the resolution experiment at 12 MPa; 35 °C and 99 mg/ml solvent concentration. The scaling in the images was prepared using the own software of the equipment.

[1] Allen, F. H. "The Cambridge Structural Database: a quarter of a million crystal structures and rising", Acta Crystallographica Section B Structural Science, 58(3), pp. 380–388, 2002.
https://doi.org/10.1107/S0108768102003890

[2] Macrae, C. F., Bruno, I. J., Chisholm, J. A., Edgington, P. R., McCabe, P., Pidcock, E., Rodriguez-Monge, L., Taylor, R., van de Streek, J., Wood, P. A. "Mercury CSD 2.0 – new features for the visualization and investigation of crystal structures", Journal of Applied Crystallography, 41(2), pp. 466–470, 2008.
https://doi.org/10.1107/S0021889807067908

[3] Karamertzanis, P. G., Anandamanoharan, P. R., Fernandes, P., Cains, P. W., Vickers, M., Tocher, D. A., Florence, A. J., Price, S. L. "(R)-1-phenylethylammonium-(R)-mandelate (PIVGEH01)", CCDC 630707: Experimental Crystal Structure Determination, 2014.
https://doi.org/10.5517/CCP59DJ

[4] Karamertzanis, P. G., Anandamanoharan, P. R., Fernandes, P., Cains, P. W., Vickers, M., Tocher, D. A., Florence A. J., Price, S. L. "Toward the Computational Design of Diastereomeric Resolving Agents: An Experimental and Computational Study of 1-Phenylethylammonium-2-phenylacetate Derivatives", The Journal of Physical Chemistry B, 111(19), pp. 5326–5336, 2007.
https://doi.org/10.1021/jp068530q

[5] de Diego, H. L. "(S)-1-phenylethylammonium-(R)-mandelate (PIVGEG)", CCDC 1234609: Experimental Crystal Structure Determination, 1994.

[6] de Diego, H. L. "Crystal Structure of (S)-1-Phenylethylammonium (R)-Mandelate and a Comparison of Diastereomeric Mandelate Salts of 1-Phenylethylamine", Acta Chemica Scandinavica, 48, pp. 306–311, 1994.
https://doi.org/10.3891/acta.chem.scand.48-0306